

Crossover Phenomena in the One-Dimensional SU(4) Spin-Orbit Model under Magnetic Fields

Yasufumi Yamashita, Naokazu Shibata*, and Kazuo Ueda

Institute for Solid State Physics, University of Tokyo, Roppongi 7-22-1, Minatoku, Tokyo 106-8666, Japan

(Received May 5, 2021)

We study the one-dimensional SU(4) exchange model under magnetic fields, which is the simplest effective Hamiltonian in order to investigate the quantum fluctuations concerned with the orbital degrees of freedom in coupled spin-orbit systems. The Bethe ansatz approaches and numerical calculations using the density matrix renormalization group method are employed. The main concern of the paper is how the system changes from the SU(4) to the SU(2) symmetric limit as the magnetic field is increased. For this model the conformal field theory predicts an usual behavior: there is a jump of the critical exponents just before the SU(2) limit. For a finite-size system, however, the orbital-orbital correlation functions approach continuously to the SU(2) limit after interesting crossover phenomena. The crossover takes place in the magnetization range of $1/3 \sim 1/2$ for the system with 72 sites studied in this paper.

I. INTRODUCTION

In recent years increasing attention has been paid to the physics related to the orbital degrees of freedom and its quantum fluctuations in the strongly correlated electron systems in addition to the charge and/or spin degrees of freedom. In the conventional treatments for the coupled spin and orbital systems, mean-field-type approaches have been used to determine an ordered orbital structure and the effects of the quantum fluctuations are usually neglected [1,2]. Recent experiments suggest, however, in some transition metal and rare earth compounds, the orbital degeneracies and quantum fluctuations of spin and orbital degrees of freedom play an important role in their unusual properties, which may require more sophisticated treatments than the mean-field approximations.

For examples, CeB₆ is known as a typical dense Kondo system ($T_K = 1 \sim 2$ K) with the Γ_8 quartet ground state, and is well known for its unique magnetic field-temperature phase diagram [3]. Since the quadrupolar ordering temperature ($T_Q \sim 3.4$ K) is of the same order as the spin Néel ordering temperature ($T_N \sim 2.3$ K), the interplay between spin and orbital quantum fluctuations may be important and thus we need to consider the effects of quantum fluctuations more seriously beyond the mean-field theories. A pure LiV₂O₄, which has a fcc normal-spinel structure and does not show any static magnetic order, is found to be the first compound which shows the heavy fermion like behavior among the transition metal oxides [4]. But its origin of the large effective mass may be different from the usual heavy-fermion systems which have nearly localized f - and itinerant conduction electrons. The highly frustrated lattice structure and nearly degenerate t_{2g} orbital at each V^{3.5+} ion are believed to be the origin of the unusual properties, such as disordered ground state and heavy-fermion like behaviors.

Generally speaking, the quantum fluctuations are less important in higher dimensions, and the classical pictures, i.e. spin and orbital ordered structures in the case

of the coupled spin and orbital models, may be applied for many cases in three dimensions. However, these experiments suggest the possibilities that the interplay between spin and orbital fluctuations destroys the classical ordered structures and the ground state may become a disordered liquid state.

In order to study the physics in which quantum fluctuations concerned with the orbital degrees of freedom are important, the SU(4) exchange Hamiltonian (1) has been considered as a prototypical model and studied extensively by several groups [5–7]. This SU(4) exchange model is derived from the highest symmetric limit of the two band Hubbard model with the strong correlation ($U/t \gg 1$) and the vanishing Hund coupling ($J = 0$) at quarter filling. The model is given by,

$$H_{\text{SU}(4)} = K \sum_{\langle i,j \rangle} \left(2\vec{S}_i \vec{S}_j + \frac{1}{2} \right) \left(2\vec{T}_i \vec{T}_j + \frac{1}{2} \right), \quad (1)$$

where $\langle i, j \rangle$ stands for a nearest neighbor pair and K is given by $2t^2/U > 0$. It consists of usual \vec{S} - and pseudo \vec{T} - spins, which describe the spin and orbital degrees of freedom, respectively. It is important to note that the both spins have the Heisenberg type isotropic interactions and the total symmetry of this model is the SU(4) group, which is higher than the apparent SU(2)⊗SU(2) group.

In one dimension, overall properties of the ground state and excitations of this most symmetric SU(4) exchange model are well understood by the previous studies [5,7–10]. In terms of the spin-ladder models, Eq.(1) corresponds to the two-leg AF Heisenberg ladder with 4-body interaction producing frustrations. A similar model without frustration (the 4-body interaction with the opposite sign) is studied by using the green's function Monte Carlo method [11]. It is noteworthy that the present model belongs to the Bethe solvable class with the general SU(N) symmetry and also belongs to the quantum critical systems with strong quantum fluctuations.

In actual systems, the highest SU(4) symmetry may be destroyed into various lower symmetries due to some anisotropies and different physics emerges depending on the way how the symmetry is lowered. In many physically relevant systems, the spin rotational invariance is approximately hold, while the SU(2) symmetry of the orbital part is easily destroyed. For example, it becomes U(1) by a single-ion anisotropy and a finite Hund coupling makes the exchange interaction of the orbital part Ising type with Z_2 symmetry [5]. Another type of symmetry lowering is the models with $SU(2)\otimes SU(2)$ symmetry which is given by Eq.(1) with arbitrary constants replaced for $1/2$. This model in one dimension is investigated both numerically and analytically by several authors [12,13].

In this paper we study the one-dimensional SU(4) exchange model under magnetic fields as another example with a lower symmetry. It is naturally expected that the quantum fluctuations in one dimension are more prominent than those in two or three dimension. Therefore one dimensional model may shed right on the role of quantum fluctuations concerned with the spin and orbital degrees of freedom. It should be also mentioned that this model is equivalent to the case with a splitting between the two orbitals. Under magnetic fields, the highest SU(4) symmetry is broken by the Zeeman splitting and the total symmetry of the model becomes $SU(2)\otimes U(1)$, where the SU(2) symmetry represents the rotational invariance of the orbital degrees of freedom and the U(1) symmetry describes the spin degrees of freedom under uniaxial magnetic fields. In sufficiently strong magnetic fields, it is evident that the all spins are fully polarized and our model reduces to the SU(2) symmetric antiferromagnetic (AF) Heisenberg model with only pseudo \vec{T} - spin degrees of freedom.

Therefore, it is interesting to investigate how the system changes from the SU(4) to the SU(2) symmetric limit as we increase the magnetic field. We study this transition by calculating the ground-state energy and elementary excitations and also by looking at the behav-

iors of the orbital-orbital correlation functions. For this purpose, we have used numerical calculations with the density matrix renormalizing group (DMRG) method as well as analytic approaches based on the Bethe ansatz and the conformal field theory (CFT). Since these methods do not introduce any uncontrolled approximations, they are suitable for investigating the effects of quantum fluctuations beyond the level of various mean-field theories.

II. GROUND STATE AND EXCITATIONS

A. Bethe ansatz equations and symmetry properties

We consider the one dimensional SU(4) exchange model with the periodic boundary conditions (PBC). First we calculate the thermodynamic ground-state energy under magnetic fields by using the Bethe ansatz methods for finite and infinite size systems. In the actual calculations, we solve the Bethe ansatz equations with specified values of the magnetization m_z , which is defined by $2S_{tot}^z/N$. In this notation, $m_z = 0$ corresponds to the SU(4) symmetric limit with no magnetic field and $m_z = 1$ corresponds to the SU(2) symmetric limit where all \vec{S} - spins order in parallel and only orbital degrees of freedom are left. The ground-state energies for the SU(4) and SU(2) symmetric limit are obtained analytically to be $1 - \pi/4 - 3 \log 2/2 \simeq -0.8251189$ and $1 - 2 \log 2 \simeq -0.3862944$, respectively [9].

Let us suppose that N_1, N_2, N_3 , and N_4 are the numbers of four species ($N = N_1 + N_2 + N_3 + N_4$ and N is the total number of sites) with the quantum numbers $(S^z, T^z) = (\uparrow, \uparrow), (\uparrow, \downarrow), (\downarrow, \uparrow)$, and (\downarrow, \downarrow) , respectively. These numbers specify the value of $S_{tot}^z = (N_1 + N_2 - N_3 - N_4)/2$ and $T_{tot}^z = (N_1 - N_2 + N_3 - N_4)/2$. We also define $M_1 = N_2 + N_3 + N_4$, $M_2 = N_3 + N_4$, and $M_3 = N_4$. The Bethe ansatz equations for the SU(4) exchange model with the quantum numbers N_1, N_2, N_3 , and N_4 are given as follows [9]:

$$\begin{aligned}
NK(\alpha_i) &= 2\pi J_{\alpha_i} - \sum_{i'=1}^{M_1} \theta(\alpha_i - \alpha_{i'}) + \sum_{j=1}^{M_2} \theta(2\alpha_i - 2\beta_j) \\
0 &= 2\pi J_{\beta_j} - \sum_{j'=1}^{M_2} \theta(\beta_j - \beta_{j'}) + \sum_{i=1}^{M_1} \theta(2\beta_j - 2\alpha_i) + \sum_{k=1}^{M_3} \theta(2\beta_j - 2\gamma_k) \\
0 &= 2\pi J_{\gamma_k} - \sum_{k'=1}^{M_3} \theta(\gamma_k - \gamma_{k'}) + \sum_{j=1}^{M_2} \theta(2\gamma_k - 2\beta_j), \tag{2}
\end{aligned}$$

where $K(\alpha) = 2 \tan^{-1}(2\alpha) \pm \pi$, $\theta(x) = -2 \tan^{-1} x$, and the suffix i, j , and k are numbered from 1 to M_1, M_2 and M_3 , respectively. For a given set of J_α, J_β , and J_γ we can calculate the parameters α_i, β_j and γ_k , so-called rapidities, by solving the $M_1 + M_2 + M_3$ coupled non-linear equations (2). The quantum numbers J_α, J_β and J_γ are integers (half integers) depending on the value of the $M_1 + M_2, M_1 + M_2 + M_3$, and $M_2 + M_3$ to be odd (even), respectively, and their distributions specify a state. The ground-state energy per site (ε_N), momentum (P), and m_z for the specified number of species, N_1, N_2, N_3 , and N_4 , are given as follows:

$$\varepsilon_N = 1 - \frac{2}{N} \sum_{i=1}^{M_1} \left\{ 1 - \cos K(\alpha_i) \right\} = 1 - \sum_{i=1}^{M_1} \frac{4}{1 + 4\alpha_i^2}, \quad (3)$$

$$P = \sum_{i=1}^{M_1} K(\alpha_i) = \frac{2\pi}{N} \left(\sum_{i=1}^{M_1} J_{\alpha_i} + \sum_{j=1}^{M_2} J_{\beta_j} + \sum_{k=1}^{M_3} J_{\gamma_k} \right), \quad (4)$$

$$m_z = n_1 + n_2 - n_3 - n_4, \quad (5)$$

where we take K as energy units hereafter, putting $K = 1$ in Eq.(1), and define $n_i \equiv N_i/N$. In order to avoid complications coming from multi-fold degeneracies [5], we only consider the system with $N = 4n$ sites (n is an integer) in the following.

Under magnetic fields, the four-fold degenerate bands in terms of the original Fermion model, are split into two doubly degenerate bands by the Zeeman effect and these two bands are labeled by spin up and down, respectively (see Fig.1). Since \vec{S} - spins are gradually polarized with the increase of magnetic fields and pseudo \vec{T} - spins are not affected directly, it is reasonable to suppose that the ground state in magnetic fields is represented by a irreducible representation with a finite S_{tot}^z and zero T_{tot}^z , which is given by the Young's diagram as illustrated in Fig.2. For $m_z = 0$ and 1, the irreducible representations of the ground state are given by the SU(4) and SU(2) singlet, respectively. For $0 < m_z < 1$, the upper and lower half rectangles represent the local SU(2) symmetry of the orbital degrees of freedom for the up and down spin bands split under magnetic fields, respectively.

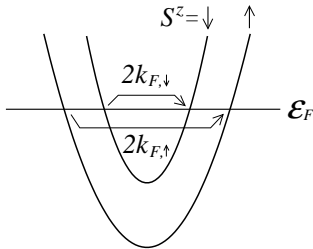


FIG. 1. Schematic band structure of the SU(4) exchange model under magnetic fields. ε_F denotes the Fermi energy.

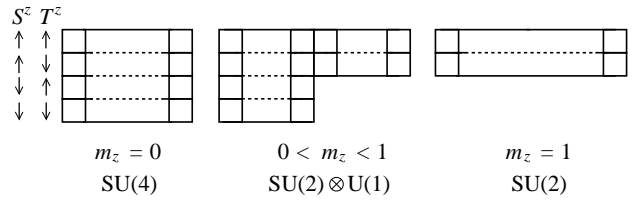


FIG. 2. The Young's diagrams for the ground states under magnetic fields. Below each diagram, magnetization and its total symmetry are given.

B. Ground-state energies under magnetic fields

We have numerically solved the coupled equations(2) under the conditions, $N_1 = N_2$ and $N_3 = N_4$, and by using Eq.(3) and (5) the ground-state energies with specified magnetization m_z are calculated for the system size $N = 100, 200$, and 400 , respectively. In order to estimate the bulk limit, we have extrapolated to the infinite system size limit by fitting these data with the function $\varepsilon_N = \varepsilon_\infty + c_1/N + c_2/N^2$. Bulk ground-state energies per site as a function of m_z are obtained as shown in Fig.3 by the solid line. The ground-state energy for the SU(4) and SU(2) symmetric limit are calculated to be -0.8251190 and -0.3862944 , which are perfectly consistent with the analytic results.

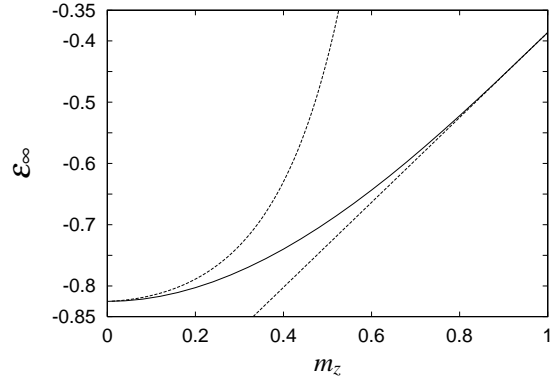


FIG. 3. Thermodynamic ground-state energy as a function of m_z . The solid line represents the ground state-energy obtained by the extrapolation to infinite system size. Broken lines stand for the asymptotic behaviors around the SU(4) and SU(2) symmetric limits.

In order to consider the thermodynamic properties of the SU(4) exchange model and to analytically obtain the asymptotic forms around the SU(4) and SU(2) symmetric limits, we take the infinite system-size limit in the Bethe ansatz equations (2) under the conditions of $N_1 = N_2$ and $N_3 = N_4$. By introducing distribution functions per unit length for the continuous rapidities α, β , and γ , we obtain the simultaneous integral equations as follows:

$$\begin{aligned}
R_1(\alpha) &= G_2(\alpha) - \frac{1}{2\pi} \int_{-\infty}^{\infty} G_1(\alpha - \alpha') R_1(\alpha') d\alpha' + \frac{1}{2\pi} \int_{-B}^B G_2(\alpha - \beta) R_2(\beta) d\beta, \\
R_2(\beta) &= -\frac{1}{2\pi} \int_{-B}^B G_1(\beta - \beta') R_2(\beta') d\beta' + \frac{1}{2\pi} \int_{-\infty}^{\infty} G_2(\beta - \alpha) R_1(\alpha) d\alpha + \frac{1}{2\pi} \int_{-\infty}^{\infty} G_2(\beta - \gamma) R_3(\gamma) d\gamma, \\
R_3(\gamma) &= -\frac{1}{2\pi} \int_{-\infty}^{\infty} G_1(\gamma - \gamma') R_3(\gamma') d\gamma' + \frac{1}{2\pi} \int_{-B}^B G_2(\gamma - \beta) R_2(\beta) d\beta,
\end{aligned} \tag{6}$$

where $G_n(x) = n/\pi(1+n^2x^2)$ and R_1 , R_2 , and R_3 are the distribution functions per unit length for the rapidities α , β , and γ , respectively. The infinite cut-off parameters except for those of β in the integral equations preserve the relations $N_1 = N_2$ and $N_3 = N_4$ and the cut-off B determines the difference between N_1 and N_3 and specifies the magnetization m_z through the relation below. The ground-state energy per site (ε_∞), the momentum P and the magnetization m_z are given by

$$\varepsilon_\infty = 1 - 2\pi \int_{-B}^B G_2(\alpha) R_1(\alpha) d\alpha, \tag{7}$$

$$P = N \int_{-B}^B K(\alpha) R_1(\alpha) d\alpha, \tag{8}$$

$$m_z = 2 \int_{|\beta|>B} R_2(\beta) d\beta. \tag{9}$$

By solving the coupled integral equations (6) numerically and using the equations (7) and (9), we may again obtain the thermodynamic ground-state energy as a function of m_z . Since there exist non-systematic errors in the procedures of discretizations for the integral equations, it is hard to calculate the ground-state energies for the SU(4) and SU(2) symmetric limits in better accuracy than 0.1% relative errors to the exact values. We have found that, for the calculation of the bulk ground state energies, Bethe ansatz method for finite-size systems with the aid of the extrapolation is more suitable than that for the infinite-size system. Since the SU(4) and SU(2) symmetric points correspond to the limits with the cut-off parameter $B = \infty$ and 0, respectively, we get analytically the asymptotic expressions of the thermodynamic ground-state energies (ε_∞) around these limits within the lowest-order calculations as follows:

$$\varepsilon_\infty \sim 1 - \frac{\pi}{4} - \frac{3 \log 2}{2} + \frac{\left(\frac{\pi}{4}\right)^2 m_z}{\left(\log \tan \frac{\pi m_z}{4}\right)^2}, \text{ (for } m_z \simeq 0), \tag{10}$$

$$\sim 1 - 2 \log 2 + \log 2 (m_z - 1), \text{ (for } m_z \simeq 1). \tag{11}$$

We also show these functions in Fig.3 by the broken lines.

C. Excitations and incommensurate soft modes

In order to obtain excited states by the Bethe ansatz method for a finite-size system, we follow the standard approach to change the distributions of integer or half-integer quantum numbers J_α , J_β , and J_γ and calculate the elementary excitations with a specified m_z . A removal, from the symmetric and continuous distributions of the quantum numbers for the ground state, creates a hole and an addition creates a particle. By creating particle-hole pair excitations corresponding to the three kinds of quantum numbers J_α , J_β , and J_γ , we can discuss three elementary massless excitations in our model. The calculated excitation spectra as a function of momentum q are shown by the solid lines in Fig.4(0)~(3) for several values of m_z . We have defined the thermodynamic limit by the extrapolation of finite-size data in the same way as for the ground-state energies and defined the momentum of the elementary excitations by the relative one to the ground state.

Figure 4 shows how the excitation spectra change between the SU(4) and SU(2) symmetric limits. In Fig.4(0), we see that three excitations have the same velocity $\pi/2$, which is consistent with the exact result obtained by Sutherland [9]. With the increase of magnetizations, the amplitudes and softening wave vectors of the two small branches of the excitations are decreased continuously and disappear at the SU(2) limit, while the largest branch approaches to the SU(2) elementary excitation. For $m_z = 1$, the model reduces to the SU(2) AF Heisenberg model of the pseudo \vec{T} -spins and its elementary excitations have been obtained to be $\pi \sin q$, which are nothing but the des Cloizeaux and Pearson modes. It is important to note that for accurate calculations of the smallest elementary excitations for larger m_z , we need calculations for larger system sizes because those excitations correspond to the rearrangements of the quantum number J_γ and its number $M_3 = N(1 - m_z)/4$ is decreased with the increase of m_z . In other words by using the Fermion model, this difficulty comes from the fact that the relative weight of the down spin band to the up spin one is decreased with the increase of m_z for a fixed system size.

The wave numbers which correspond to the incommen-

surate soft modes in the elementary excitations (Fig.4) are specified by the nesting vectors of the Fermi points in Fig.1 as follows: $2k_{F,\downarrow} = \pi(1 - m_z)/2$, $4k_{F,\downarrow} = \pi(1 - m_z)$, and $2k_{F,\uparrow} = \pi(1 + m_z)/2$. Since the relation $4k_{F,\downarrow} \equiv 4k_{F,\uparrow} \pmod{2\pi}$ is always satisfied, the $4k_{F,\uparrow}$ mode is not independent. We have found that the excitation spectrum with the softening at $q = 2k_{F,\downarrow}$ ($2k_{F,\uparrow}$) correspond to the kink-type excitations of the orbital pseudospin \vec{T} in the down (up) spin band and the spectrum with the softening at $q = 4k_{F,\downarrow}$ corresponds to the kink-type \vec{S} -spin excitations, so-called spinons.

It may be worth to mention that the shift of the momentum of the singularity in the structure factor is actually observed for the SU(2) spin case. Dender *et.al.* [14] have studied the copper benzoate, $\text{Cu}(\text{C}_6\text{D}_5\text{COO})_2 \cdot 3\text{D}_2\text{O}$, which is known to be the typical spin 1/2 one-dimensional antiferromagnet, by the neutron scattering experiment and have found the existence of the field-induced soft modes at the wave vector $q = \pi \pm 2\pi M(H)/g\mu_B$, which is consistent with the Bethe ansatz solutions.

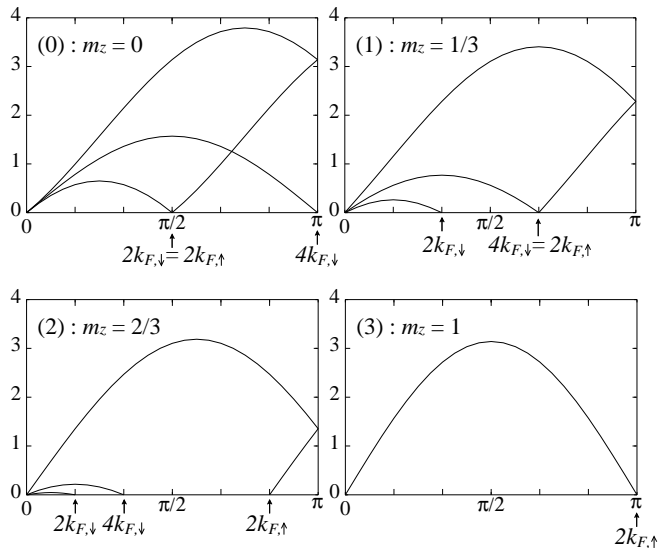


FIG. 4. Dispersion relations in the infinite-size system limit for several values of m_z . The vertical and horizontal axis represent the energy and momentum, respectively. Below each figure, we label the incommensurate soft modes in terms of the original fermion model.

III. CROSSOVER PHENOMENA OBSERVED IN ORBITAL-ORBITAL CORRELATION FUNCTIONS

A. Correlation functions in real space

In this section, we investigate the orbital-orbital correlation functions under magnetic fields by the numerical calculations using the DMRG method [15]. Since the

DMRG method is more suitable for open boundary conditions (OBC) than PBC, we employ the OBC in order to carry out the calculations for large system sizes with sufficient accuracy. We consider the 72-site system and obtain the correlation functions up to the distance of 36 sites. As usual we calculate the wave function of the system with a specified S_{tot}^z instead of dealing with the model under magnetic fields. To eliminate the oscillations coming from the open boundaries, we define the averaged orbital-orbital correlation functions as follows:

$$\langle T_i^z T_{i+j}^z \rangle \equiv \frac{1}{4} \sum_{k=0}^3 \langle T_{i+k}^z T_{i+k+j}^z \rangle \quad (12)$$

We have confirmed that after this averaging procedure the i dependences of the correlation functions are almost removed. The obtained correlation functions are shown in Fig.5 for $m_z = 0, 1/3, 1/2, 5/6$, and 1.

For general models with the SU(N) symmetry, the asymptotic behavior of the correlation functions have been obtained in a simple form by Affleck [10]. When we apply his results to our model with the SU(4) or SU(2) symmetric limit, which corresponds to $m_z = 0$ or 1, respectively, the orbital-orbital correlation functions behave asymptotically as follows:

$$\langle T_i^z T_{i+j}^z \rangle = A_0 \left(\frac{\cos(2\pi j/N + \varphi_0)}{j^\alpha} + \frac{1}{j^\beta} \right),$$

where A_0 and φ_0 are non-universal constants depending on each model, while the critical exponents $\alpha = 2(1 - 1/N)$ and $\beta = 2$ are universal constants. For the SU(4) symmetric limit, we try to fit the data from $j = 18$ to 32 with this asymptotic form by the least mean square method. We do not use the data for $j > 32$, because these sites are so close to the boundary that they are affected by the oscillations from the open boundary even after the averaging procedures. From the fitting we get the critical exponents to be $\alpha = 1.52 \pm 0.08$, and $\beta = 2.02 \pm 0.08$. These exponents are consistent with the analytic results by Affleck. For the other limit with the SU(2) symmetry, we similarly estimate the critical exponents for the oscillating term with wave vector $q = \pi$ and non-oscillating term to be 1.04 ± 0.01 and 2.5 ± 0.6 , respectively, neglecting the logarithmic corrections. These results are again consistent with the exact values 1 and 2. In this fitting analysis, we have used the data from $j = 18$ to 25 in order to eliminate the boundary effect, which is considered to be more noticeable than that for the SU(4) limit because the critical exponent of the SU(2) limit is smaller than that of SU(4).

For the intermediate magnetizations between the SU(4) and SU(2) symmetric limits, we can not get meaningful results concerned with the exponents from a similar fitting as the SU(4) or SU(2) limit, since the correlation functions have more complicated structure as is shown in Fig.5. However, the correlation functions in real space show interesting behaviors as the SU(2) symmetric limit is approached. First of all, let us take a look

at Fig.5 paying attention to their periodicities and how they approach to the SU(2) limit. For a small value of m_z , we see clear periodic oscillations with the wave vectors $2k_{F,\downarrow}$ and $2k_{F,\uparrow}$ (see Fig.5(a) and (b)), which correspond to the incommensurate soft modes of the excitation spectrum discussed in the previous section. As we increase magnetic fields, the correlation functions approach to the SU(2) one (Fig.5(e)) in such a way as the number of periodic structures observed within the 36-site length is decreased and at the same time the SU(2)-like structure with the wave vector π becomes noticeable (Fig.5(c) and (d)). These behaviors are consistent with the fact in the elementary excitations, that $2k_{F,\downarrow}$ and $4k_{F,\downarrow}$ soft modes vanish and the $2k_{F,\uparrow}$ soft modes continuously evolve to the des Cloizeaux and Pearson modes at π with the increase of magnetic fields. We have also found that for a large value of m_z , the correlation functions are well-illustrated by the following pictures where the oscillations with the wave vector π are modulated by the slowly-varying $2k_{F,\downarrow}$.

With the increase of m_z , the period of the $2k_{F,\downarrow}$ oscillations becomes longer and the region, where the SU(2)-like behaviors with wave vector π are dominant, becomes more extended, and in the end for $m_z = 1$, the correlation functions become the true SU(2) ones. In this way, the bigger the value of m_z is, the more distant becomes the asymptotic region, which is governed by the envelope of $2k_{F,\downarrow}$ oscillations, and the more prominent are the SU(2)-like behaviors within the envelope. Generally speaking, as long as we consider a finite-size system, the calculated correlation functions do not reach the asymptotic region for a larger value of m_z than some critical magnetization, which is an increasing function of the system size, and the crossover phenomena from the SU(4) to the SU(2) symmetric limit take place. Beyond this characteristic magnetization the SU(2)-like behaviors with the slowly-varying envelope described by the $2k_{F,\downarrow}$ oscillations are a better picture for the calculated correlation functions in a finite length than the asymptotic behaviors of the $2k_{F,\downarrow}$ and $2k_{F,\uparrow}$ oscillations.

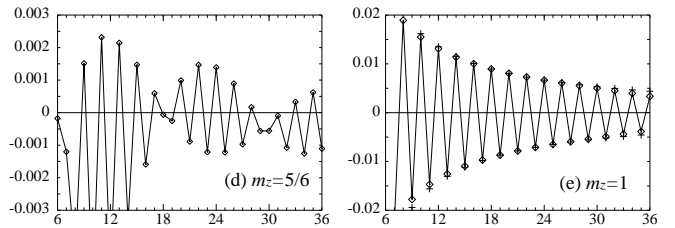
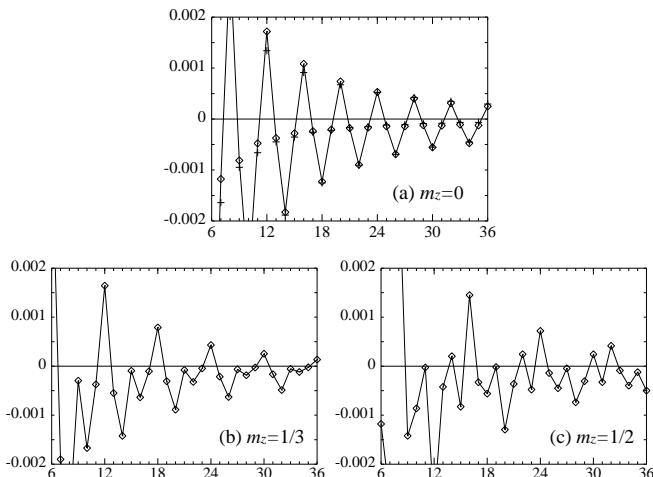


FIG. 5. Orbital-orbital correlation functions $\langle T_i^z T_{i+j}^z \rangle$ as a function of j for the 72-site system with $m_z = 0, 1/3, 1/2, 5/6$ and 1. In figures (a) and (e), we plot the fitting results by the symbols +.

B. Correlation functions in momentum space and asymptotic behaviors

Since we want to minutely observe the transition from the SU(4) to the SU(2) symmetric limit with the increase of the magnetic field, next we focus on the asymptotic behavior of the correlation functions and concretely estimate the crossover region between these two limits for a finite-size system with 72-site length. For this purpose, we discuss the anomalies of the structure factors by calculating the fourier transformation which is defined by

$$T^z(q) \equiv \sum_{j=-N/2+1}^{N/2} \langle T_i^z T_{i+j}^z \rangle e^{-iqj} \quad . \quad (13)$$

In this definition, we have periodically arranged the numerically calculated correlation functions up to $N/2$ -site length to form the ring with the N sites, which are less affected by boundary effects, and defined the structure factors for the ring. The obtained structure factors for the 72-site system by changing m_z from 0 to 1 by $1/6$ are shown in Fig.6. In the figure we see clear two singular cusp structures at $q = 2k_{F,\downarrow}$ and $2k_{F,\uparrow}$. These dominant cusps correspond to the field-induced soft modes in the dispersion relations obtained in the previous section, and may be interpreted as the orbital excitations in the down and up spin bands as illustrated in Fig.1. It is important to note that the $q = 4k_{F,\downarrow}$ ($\equiv 4k_{F,\uparrow} \pmod{2\pi}$) mode does not appear in the orbital-orbital correlation functions. This is because the excitation with $q = 4k_{F,\downarrow}$ is considered to be an excitation with the spin currents. In fact the $4k_{F,\downarrow}$ ($4k_{F,\uparrow}$) momentum transfer comes from such excitations as we move two particles from the left Fermi point of the down (up) spin band to the right one. This situation is completely analogous to the case of the one-dimensional Hubbard model, where the both $2k_F$ and $4k_F$ oscillating parts appear in the density-density correlation function, while the $4k_F$ part is absent in the spin-spin correlation functions because the dominant oscillating term with $q = 4k_F$ originates from the holon excitations [16].

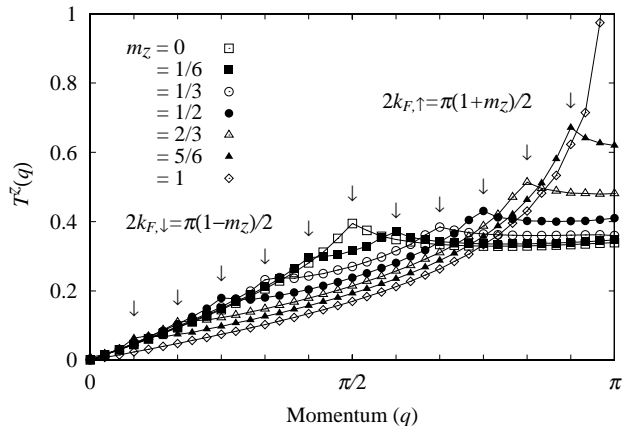


FIG. 6. Fourier transform of the orbital-orbital correlation functions for $m_z = 0, 1/6, 1/3, 1/2, 2/3, 5/6,$ and 1 . We label the wave numbers $2k_{F,\downarrow}$ and $2k_{F,\uparrow}$ by the down arrows (\downarrow) for each m_z . $T^z(\pi)$ for $m_z = 1$ (which is out of the plot range) is equal to 1.486 .

According to the conformal field theory [17], the critical exponents α_1 , α_2 , and α_3 which correspond to the oscillating terms with $q = 2k_{F,\downarrow}$, $4k_{F,\downarrow}$, and $2k_{F,\uparrow}$, respectively, are obtained as follows:

$$\alpha_1 = \alpha_3 = 1 + \frac{\xi^2}{2} \equiv \alpha, \quad \alpha_2 = 2\xi^2 = 4(\alpha - 1),$$

where ξ is defined by $\xi(\beta = B)$ and $\xi(\beta)$ is obtained by the following integral equation:

$$\xi(\beta) = 1 + \int_{-B}^B d\beta' \xi(\beta') \left[\frac{1}{2\pi} \int_{-\infty}^{\infty} dx \frac{1 - e^{-|x|}}{1 + e^{|x|}} e^{ix(\beta - \beta')} \right].$$

We calculate these critical exponents as a function of m_z , where m_z is given by Eq.(9), which only depends on B . The obtained results are shown in Table I. In the table, we represent the limit to unity from $m_z < 1$ by 1-0. The critical exponent α is equal to 1.5 at $m_z = 0$ and 1-0 and continuously changes between $0 < m_z < 1$ with larger values about $1.5 \sim 1.6$ and jumps to 1 at the SU(2) symmetric point with $m_z = 1$. In Fig.6, the left and right cusp structures correspond to the modes with the critical exponent α_1 and α_3 , respectively. Though the conformal field theory predicts the same critical exponent for the both cusps, the calculated structure factors seem to be quite different, especially for large m_z . Apparently the left side cusps become less dominant, while the right side cusps are more prominent as the increase of m_z .

In order to consider possible reasons, we again employ the schematic band structure of the original fermion model shown in Fig.1. As the increase of applied magnetic field, it is evident that the relative weight of the down spin band is diminished as mentioned in Sec.II C. It is the reason that the left hand side cusp structures are suppressed and their amplitudes become smaller in contrast to the predictions by the CFT. By a closer look

at the right side cusp structures, it is found that until the value of m_z less than about $1/3$, the cusp shows a little weaker anomaly than that for $m_z = 0$, which is consistent with the prediction by the CFT, while for the region of $m_z > 1/2$ the cusps grow rapidly and seem to continuously develop into the SU(2) AF cusp structure with the critical exponent 1 .

These characteristic features of the Fourier transformed orbital-orbital correlation functions for the system with 72 sites are explained by the crossover phenomena due to the finiteness of the system and do not contradict the CFT predictions. It is reasonable to consider that in the region $m_z > 1/2$ the relative weight of the down spin band is so small and the $2k_{F,\downarrow}$ oscillations have such a long period that the calculated correlation functions do not reach the asymptotic region within the 72-site length and show the properties of the single up spin band which contribute relatively large weight, that is the SU(2)-like behavior in the envelope of the $2k_{F,\downarrow}$ oscillation. Therefore the cusp structures seem to continuously evolve into the behavior of the SU(2) AF Heisenberg model. On the other hand for $m_z < 1/3$ both upper and lower split bands have significant weight and $2k_{F,\downarrow}$ and $2k_{F,\uparrow}$ are not so small that the calculated correlation functions are in the asymptotic region and they show the asymptotic behaviors of the SU(4) exchange model under the magnetic field predicted by the CFT. This picture is also consistent with the behaviors of the real-space correlation functions in which the SU(2)-like behaviors become noticeable around $m_z = 1/2$.

To summarize, for small m_z the orbital-orbital correlation functions show the oscillations with the wave vectors $2k_{F,\downarrow}$ and $2k_{F,\uparrow}$, which give a consistent picture with the prediction by the CFT. For the understanding of the region with large m_z , however, we find it useful and appropriate to rewrite these two oscillating term as $\cos(2k_{F,\downarrow}j)$ and $\cos(2k_{F,\uparrow}j) = \cos(\pi j) \times \cos(2k_{F,\downarrow}j)$. The second equation, which comes from the relation $2k_{F,\downarrow} + 2k_{F,\uparrow} = \pi$ originating from the quarter filling, gives for the correlation functions of large m_z a simple picture in which the SU(2)-like oscillations with the wave vector π are modulated by the slowly-varying $2k_{F,\downarrow}$ oscillations. Following this picture, we may understand straightforwardly how a finite-size system continuously makes a transition from the SU(4) to the SU(2) symmetric limit as we increase magnetic fields. In particular, the continuous growth of the cusp structure into the SU(2) limit shown in Fig.5 does not contradict the prediction by the CFT: a jump of the critical exponent between $m_z = 1-0$ and 1 .

TABLE I. The critical exponent α for the magnetizations m_z from 0 to 1 by $1/6$.

m_z	0	1/6	1/3	1/2	2/3	5/6	1-0	1
α	1.500	1.562	1.581	1.585	1.573	1.543	1.500	1.000

IV. CONCLUSIONS AND DISCUSSIONS

In summary, we have investigated the SU(4) exchange model, which describes the strong quantum fluctuation limit of the two band Hubbard model, under magnetic fields and observed how the system transforms from the SU(4) symmetric limit with zero magnetization to the fully polarized SU(2) limit by using the Bethe ansatz method and DMRG calculations of the orbital-orbital correlation functions. First of all, we have kept the trace of the ground-state energy as a function of m_z and also obtained the analytic forms around the SU(4) and SU(2) symmetric limits. In order to study low energy properties of this model, we calculated three independent elementary excitations by the standard Bethe ansatz technique and found the field-induced incommensurate soft modes. Through the DMRG calculations of the orbital-orbital correlation functions under magnetic fields, we have found that the $2k_{F,\downarrow}$ and $2k_{F,\uparrow}$ modes, which carry the orbital pseudospin currents, give rise to dominant cusp structures, while the $4k_{F,\downarrow}$ mode, which carries the spin current, does not appear in the structure factors. We also conclude that for a finite-length system the crossover phenomena take place in the different way predicted by the CFT, and after that the correlation functions are properly described by the SU(2)-like behavior with the slowly-varying envelope of the $2k_{F,\downarrow}$ oscillations. As m_z approaches to unity, the period of envelope becomes longer and longer and thus the calculated finite-length correlation functions seem to continuously change into the SU(2) ones for a finite size. Corresponding to this fact, the cusp structures at the $2k_{F,\uparrow}$ observed in the structure factors develops into the SU(2) ones continuously without showing any jumps of the critical exponents. By comparing the calculated results and the CFT results, we estimate the crossover region between the SU(4) and the SU(2) symmetric limits to be $1/3 \sim 1/2$ when we consider the relatively short length system of 72 sites. It should be noted that from the symmetry of \vec{S}^- and \vec{T}^- spin degrees of freedom, we expect similar results for the spin-spin correlation functions under uniaxial pressures or crystal fields produced by single-ion anisotropies. Under the anisotropies, one type of orbital of the two is preferred and the four-fold degenerate bands split into the two doubly degenerate bands depending on the $T^z = \pm 1/2$.

Lastly, we would like to briefly comment on the relevance of the apparent difference in the crossover phenomena between the calculated correlation functions and the correlation exponents predicted by the CFT. Let us take the example of $m_z = 5/6$ shown in Fig.5(d). The $2k_{F,\downarrow} = \pi/12$ oscillation has the period of 24 sites, and thus it is reasonable to assume that it require a few hundreds sites to reach the asymptotic region. From the CFT analysis, we can get the informations about the mathematically exact asymptotic behaviors for the infinite sys-

tem size. In the real materials, however, perfect spin system cannot be realized and even for very pure systems their intrinsic length, where the exact one dimensionality are kept without any structural defects or impurities, would be some hundred atomic lengths at most. Therefore the results discussed in the present paper serve a simple example where the crossover phenomena in real systems may be different from the one predicted by the CFT. In this sense, it is necessary to pay some attention for the application of the CFT results to realistic finite-length systems.

ACKNOWLEDGMENTS

We are grateful to Norio Kawakami for many helpful comments and discussions.

-
- * Present address: Institute of Materials Science, University of Tsukuba, Tsukuba 305, Japan.
- [1] K. I. Kugel and D. I. Khomskii, Sov. Phys. JETP **37**, 725 (1973) [Zh. Eksp. Teor. Fiz. **64**, 1429 (1973)].
 - [2] S. Inagaki, J. Phys. Soc. Jpn. **39**, 596 (1975).
 - [3] J. M. Effantin, J. Rossat-Mignod, P. Burlet, H. Bartholin, S. Kunii and T. Kasuya, J. Magn. Magn. Mater. **47 & 48**, 145 (1985).
 - [4] S. Kondo, D.C. Johnston, C.A. Swenson, F. Borsa, A.V. Mahajan, L.L. Miller, T. Gu, A.I. Goldman, M.B. Maple, D.A. Gajewski, E.J. Freeman, N.R. Dilley, R.P. Dickey, J. Merrin, K. Kojima, G.M. Luke, Y.J.Uemura, O.Chmaissem, and J.D.Jorgensen, Phys. Rev. Lett. **78** 3729, (1997).
 - [5] Y. Yamashita, N. Shibata, and K. Ueda, Phys. Rev. B **58**, 9114 (1998)
 - [6] Y. Q. Li, Michael Ma, D. N. Shi, and F. C. Zhang, Phys. Rev. Lett. **81** 3527 (1998)
 - [7] B. Frischmuth, F. Mila, and M. Troyer, Phys. Rev. Lett. **82**, 835, (1999).
 - [8] Y. Q. Li, F. C. Zhang, Michael Ma, and D. N. Shi, LANL cond-mat/9902269.
 - [9] B. Sutherland, Phys. Rev. B **12**, 3795 (1975).
 - [10] I. Affleck, Nucl. Phys. B **265**, 409 (1986).
 - [11] L. Guidoni, G. Santoro, S. Sorella, A. Parola, and E. Tosatti, LANL cond-mat/9809013.
 - [12] S. Pati and R. Singh, Phys. Rev. Lett **81**, 5406 (1998)
 - [13] P. Azaria, A. Gogolin, P. Lecheminant, and A. Nersesyan, LANL cond-mat/9903047.
 - [14] D. Dender, P. Hammar, D. Reich, C. Broholm, and G. Aeppli, Phys. Rev. Lett **79**, 1750 (1997)
 - [15] S. R. White, Phys. Rev. Lett. **69**, 2863 (1992), and S. R. White, Phys. Rev. B **48** 10345 (1993).
 - [16] N. Kawakami and S. Yang, J. Phys., Condens. Matter **3**, 5983 (1991)
 - [17] T. Itakura and N. Kawakami, J. Phys. Soc. Jpn. **64**, 2321 (1995)